Identification of a Stability Determinant on the Edge of the Tet Repressor Four-Helix Bundle Dimerization Motif†

Peter Schubert, Dirk Schnappinger, Klaus Pfleiderer, and Wolfgang Hillen*

Lehrstuhl für Mikrobiologie, Institut für Mikrobiologie, Biochemie und Genetik, Friedrich-Alexander-Universität Erlangen−Nürnberg, Staudtstrasse 5, 91058 Erlangen, Germany

Received August 15, 2000; Revised Manuscript Received October 25, 2000

ABSTRACT: Isofunctional tetracycline repressor (TetR) proteins isolated from different bacteria show a sequence identity between 38 and 88% of the residues. Their active state is a homodimer formed by a four-α-helix bundle as the main interaction motif. We utilize this sequence variation of isofunctional proteins to determine residues contributing to the stability of the four-helix bundle. The thermodynamic stabilities of two TetR proteins with 63% sequence identity were determined by urea-induced reversible denaturation followed by fluorescence and circular dichroism. Both methods yield identical results. The $\Delta G°_U$ (H_2O) values are 60 and 75 kJ mol^{-1}. We have constructed TetR hybrid proteins derived from these wild types to identify the determinant leading to the 15 kJ mol^{-1} stability difference. Successive size reduction of the exchanged portion yielded two single residues affecting the overall protein stability. The P184Q exchange leads to a more stable protein, whereas the G181D exchange located at the solvent's exposed edge of the four-helix bundle is solely responsible for the reduced stability. Additional mutants based on crystal structures of TetR do not reveal any hint for steric interference of the Asp181 side chain with neighboring residues. Thus, this is an example for the role played by surface-exposed turn residues for the stability of four-helix bundles. We assume that the larger conformational flexibility of Gly and the reduction of the negative surface charge could favor formation of the turn on the edge of the four-helix bundle.

Protein−protein interactions are of crucial importance for many biological processes such as cell−cell interaction, signal recognition, and transduction. The specific assembly of polypeptides into protein complexes occurs, furthermore, in many enzymes, DNA and RNA binding proteins, and larger nucleoprotein complexes. Thus, the recognition among polypeptides to form higher order structures is as essential for many activities as the recognition of substrates or DNA and RNA sequences. In addition, the interaction between subunits is also important for correct folding of many polypeptides (*1*) because the monomeric subunits are often unstable (*2*); some are only detectable when assembled within complexes (*3*). There is only a limited set of structural motifs for protein−protein interaction known to date, among them leucine zippers (*4*) and four-helix bundles (*5*). Interactions between residues in these conserved structural elements can contribute to the recognition of subunits and/or the thermodynamic stability of protein complexes (*6*, *7*).

The mechanistic details governing recognition and affinity of protein oligomerization by four-helix bundles are only poorly understood. We have previously employed the naturally occurring Tet repressor sequence variants, which dimerize by four-helix bundles, to determine residues important for protein−protein recognition in this motif (*8*, *9*). In this paper, we describe two residues which alter the thermodynamic stability of the tetracycline repressor (TetR) four-helix bundle.

TetR variants are homodimers which regulate the expression of tetracycline (tc) resistance genes in Gram-negative bacteria in response to the presence of tc (*10*). On the basis of sequence similarities, the isolates from various bacteria have been grouped into nine classes called TetR(A) to TetR(E), TetR(G), TetR(H), TetR(J), and TetR(30) (*11*). The proteins share between 38 and 88% sequence identity. The crystal structures of TetR(D) in different functional states (*12*−*14*) revealed that a four-helix bundle mediates dimerization. It is formed by the helices α8 and α10 intersected at an angle of ∼80° in an antiparallel fashion with the symmetry-related helices α8′ and α10′ of the other subunit (*15*). The complete subunit interaction area formed by helices α6−α10 is flat and covers about 27% of the total accessible surface. Intertwining of the polypeptide chains such as in a Trp repressor does not occur (*16*).

We have determined the thermodynamic stability of TetR(D), which is less stable by 15 kJ mol^{-1} than the sequence variant TetR(B) (*17*). The construction and use of the TetR(B/D) chimera led to the identification of one residue responsible for the different thermodynamic stabilities in these variants. Possible underlying mechanisms are discussed.

EXPERIMENTAL PROCEDURES

Materials and General Methods. Anhydrotetracycline (atc) was purchased from Acros (Geel, Belgium), and all other

† This work was supported by the Deutsche Forschungsgemeinschaft through SFB 473 and the Fonds der Chemischen Industrie (FCI).

* To whom correspondence should be addressed. Phone: +49 9131 85 28081. Fax: +49 9131 85 28082. E-mail: whillen@biologie.uni-erlangen.de.

10.1021/bi001927e CCC: $20.00
Published on Web 02/17/2001

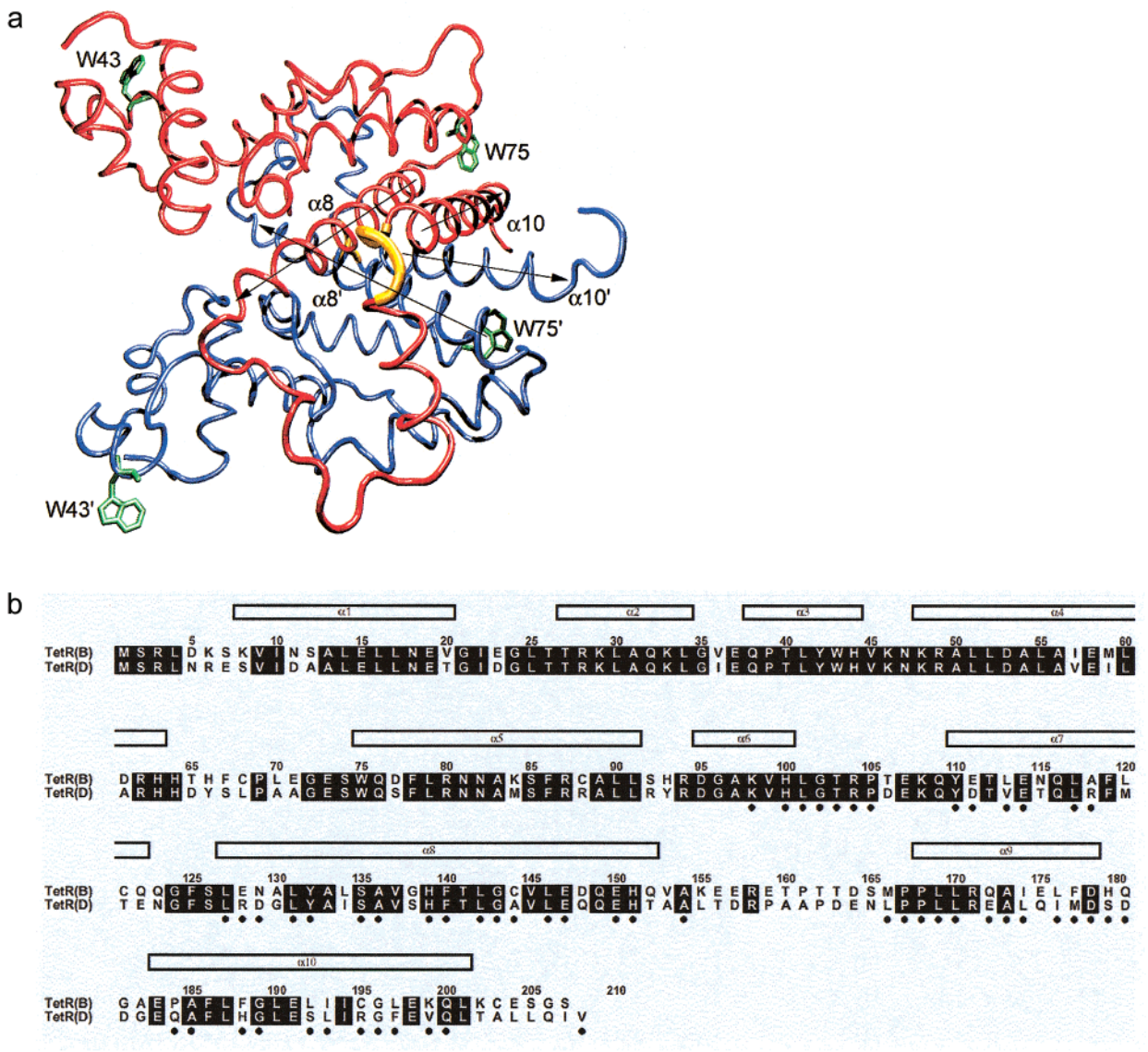

FIGURE 1: Crystal structure of TetR(D) and alignment of TetR(B) and TetR(D) sequences. (a, top) Crystal structure of TetR(B/D): monomers are depicted as blue and red ribbons, respectively, W43 and W75 in the two monomers are indicated as green residues, and the turn 179−183 is highlighted in yellow using the VMD program (*34*). The helices α8, α8′, α10, and α10′ are indicated by arrows. (b, bottom) Alignment of TetR(B) and TetR(D) sequences. Conserved amino acids are shown in inverse print. Residues involved in forming the dimerization surface (taken from ref *8*) are marked with a black dot below the sequence.

chemicals are from Merck (Darmstadt, Germany), Roth (Karlsruhe, Germany), or Sigma (München, Germany) at the highest available purity. Enzymes for DNA restriction and modification are from New England Biolabs (Schwalbach, Germany), Boehringer (Mannheim, Germany), Stratagene (Heidelberg, Germany), or Pharmacia (Freiburg, Germany). Oligonucleotides were obtained from PE Applied Biosystems (Weiterstadt, Germany). Sequencing was carried out according to the protocol provided by Perkin-Elmer for cycle sequencing and analyzed with an ABI PRISM 310 genetic analyzer (PE Applied Biosystems, Weiterstadt, Germany).

Bacterial Strains and Plasmids. All bacterial strains are derived from *Escherichia coli* K12. Strain DH5α [*hsdR*17(r_k^-,m_k^+), *recA*1, *endA*1, *gyrA*96, *thi*, *relA*1, *supE*44, *ϕ*80d*lacZ*Δ*M*15, Δ(*lacZYA-argF*)U169] was used for general cloning procedures and strain RB791 [IN(*rrnD-rrnE*)1, $lacI^qL_8$] (*18*) for overexpression of TetR. Strain WH207 [Δ*lacX*74, *galK*, *rpsL*, *thi*, *recA*13] (*19*) served as host strain for *β*-galactosidase assays. The plasmids pWH1200 (*20*), pWH520Δ9-11 (*21*), pWH806, and pWH853 (*19*) as well as pWH1950 (*22*) have previously been described.

Construction of the Chimeric TetR Genes. All TetR variants were constructed by polymerase chain reaction (PCR) according to the three-primer method (*23*). The products of the second PCR reaction were purified and digested with *Xba*I/*Mlu*I or *Mlu*I/*Nco*I and cloned into likewise digested pWH853 to replace the respective portion of TetR. For overexpression, these constructs were digested with *Xba*I and *Nco*I and cloned into pWH1950. Positive candidates were analyzed by sequencing of tetR.

β-Galactosidase Assays. Repression and induction of the TetR variants as well as the negative transdominance of TetR(B)Δ9−11 and TetR(D)Δ9−11 were assayed in *E. coli* WH207*λtet50* carrying the respective pWH853 derivatives. The phage *λtet50* contains a *tetA-lacZ* transcriptional fusion (*24*) integrated as a single copy into the WH207 genome.

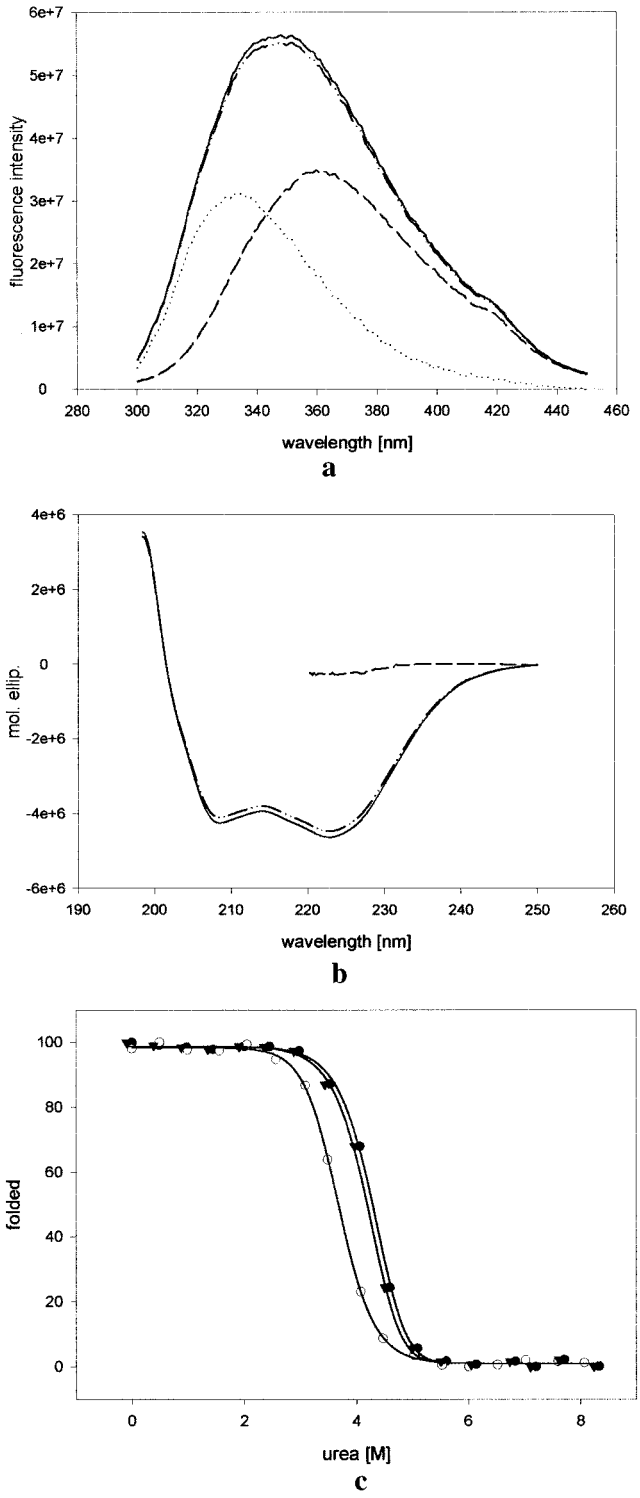

FIGURE 2: Denaturation of TetR(D) observed by fluorescence and CD. (a) Fluorescence emission spectra of native (—), denatured (– –), and renatured (—••—) TetR(D). The dotted curve (•••) represents the difference between the spectra of the native and denatured forms. (b) CD spectra of native (—), denatured (– –), and renatured (—••—) TetR(D). (c) Urea-induced denaturation curves of TetR(D) (open dots), TetR(D)Asp181Gly (filled triangles), and TetR(B) (filled dots) determined by the change of fluorescence.

Bacteria were grown in LB at 28 °C, supplemented with the appropriate antibiotics, and 0.2 μg mL^{-1} atc in overnight and log phase cultures for induction. β-Galactosidase activities were determined as described by Miller (*25*). Three independent cultures were assayed for each strain, and measurements were repeated at least twice.

Table 1: Thermodynamic Stabilities of TetR(B) and TetR(D) Determined by Urea-Dependent Denaturation

	fluorescence[a]				CD[b]	
	1 μM		5 μM		5 μM	
	$\Delta G°_U(H_2O)$ [kJ mol^{-1}]	$urea_{1/2}$ [M]	$\Delta G°_U(H_2O)$ [kJ mol^{-1}]	$urea_{1/2}$ [M]	$\Delta G°_U(H_2O)$ [kJ mol^{-1}]	$urea_{1/2}$ [M]
TetR(B)	75 ± 5	4.3	78 ± 5	4.8	76 ± 4	4.7
TetR(D)	60 ± 3	3.8	61 ± 3	4.2	63 ± 5	4.3

[a] Unfolding was followed by the change of fluorescence at 330 nm, using protein concentrations of 1 μM (excitation at 280 nm) or 5 μM (excitation at 295 nm). The relationship is given by $urea_{1/2} = -[RT \ln P_t + \Delta G°_U(H_2O)]/m$, with R being the gas constant, T the absolute temperature, P_t the total protein concentration, and m the slope of the plot of $\Delta G°_U$ vs denaturant concentration. [b] The change of the CD signal was observed at 222 nm.

Table 2: Repression, Induction, and in Vitro Thermodynamic Stabilities of TetR Variants

	repression β-gal [%]	inducibility[a] β-gal [%]	$urea_{1/2}$[b] [M]
TetR(D)	8.8 ± 0.3	64 ± 1.7	3.8
TetR(B/D)110−208	0.9 ± 0.0	43 ± 1.2	3.7
TetR(B/D)123−208	0.7 ± 0.0	43 ± 0.1	3.8
TetR(B/D)168−208	1.3 ± 0.1	46 ± 1.3	3.9
TetR(B/D)179−208[c]	1.1 ± 0.1	47 ± 2.1	4.0
TetR(B/D)188−208	1.2 ± 0.0	51 ± 3.4	4.4
TetR(B/D)192−208	1.1 ± 0.0	49 ± 2.2	4.2
TetR(B)	1.4 ± 0.1	96 ± 1.3	4.3
TetR(B/D)179−184[c]	1.1 ± 0.0	59 ± 2.6	4.4
TetR(B/D)180−184	1.3 ± 0.0	60 ± 2.8	4.3
TetR(B/D)181−184	1.1 ± 0.1	55 ± 2.6	4.4
TetR(B/D)182−184	1.1 ± 0.1	52 ± 2.0	4.9
TetR(B/D)181	1.7 ± 0.3	57 ± 2.9	3.9
TetR(D/B)181	10.0 ± 1.1	61 ± 0.7	4.2
TetR(B/D)184	1.3 ± 0.1	62 ± 2.4	4.9
TetR(D/B)184	14.1 ± 1.4	62 ± 3.1	3.1
TetR(D)Q148A	nd[d]	nd	3.8

[a] Induction was determined at 0.2 μg mL^{-1} atc. The 100% expression level of β-galactosidase corresponds to 9170 ± 460 units determined in *E. coli* WH207λ*tet50*. [b] $Urea_{1/2}$ values of the chimeric TetR variants were calculated from the change of fluorescence at 330 nm excited at 280 nm at 22 °C. [c] Constructs were taken from ref *8*. [d] nd: not determined

Purification of TetR Variants. pWH1950 derivatives containing the desired TetR mutants were transformed into *E. coli* RB791. Cells were grown in 3 L of LB at 28 °C in shaking flasks. The TetR expression was induced by adding isopropyl-1-thio-β-D-galactopyranoside (IPTG) to a final concentration of 1 mM at an OD_{600} of 0.7−1.0. Cells were pelleted, resuspended in buffer A (50 mM NaCl, 2 mM dithiothreitol, and 20 mM sodium phosphate of pH 6.8), and broken by sonication, and TetR variants were then purified by cation-exchange chromatography and gel filtration as described (*22*). The activities of the proteins were determined by titration with atc (*26*), and the amounts were obtained from the UV absorption at 280 nm (*27*).

Unfolding of TetR Variants. We used F buffer (100 mM Tris-HCl of pH 7.5, 100 mM NaCl, 5 mM $MgCl_2$, 1 mM EDTA, and 1 mM dithiothreitol) for all denaturation measurements. Urea was obtained from ICN Biochemicals (Eschwege, FRG), and urea solutions were freshly prepared every day. Equilibrium denaturation was performed by incubating protein samples overnight at the indicated urea concentrations. Renaturation reactions were achieved by incubating the samples overnight at 8 M urea and then

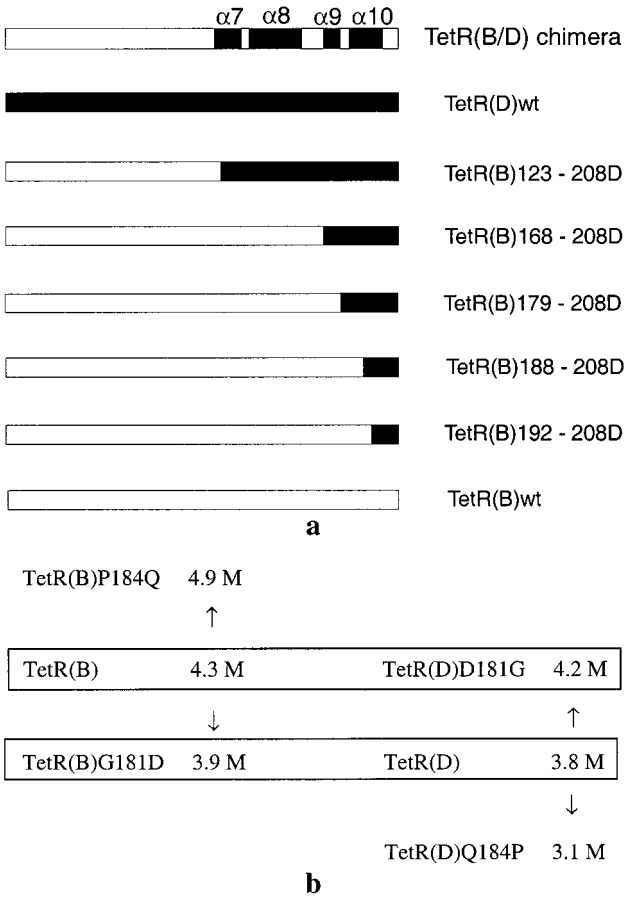

FIGURE 3: Chimeric TetR variants constructed from the B and D wild types. (a) Overview of the chimeric TetR(B/D) constructs. The respective wild-type proteins are shown by filled (TetR(D)) and open (TetR(B)) bars. The hybrid proteins are shown with their designation given on the right side. The top panel indicates the location of the helices α7−10 in TetR. (b) Overview over the mutant TetR proteins with exchanges at positions 181 and 184 and their thermodynamic stabilities given in molar urea of the transition midpoint.

diluting them 200-fold with F buffer. All reactions were performed at 22 °C, and all TetR concentrations are given as monomer. Thermodynamic calculations of the urea-induced denaturation of the TetR variants were done as described before (*17*).

Fluorescence and Circular Dichroism (CD) Spectroscopy. Fluorescence intensities were measured in a Spex Fluorolog 1680 double spectrometer using 1 cm cells at protein concentrations of 1 or 5 μM. Excitation was set to 280 nm at 1 μM TetR and to 295 nm at 5 μM TetR. The bandwidth for excitation and emission was 4 nm. CD measurements were carried out in a Jasco J-715 spectropolarimeter at protein concentrations of 5 μM in 0.5 cm cells.

RESULTS AND DISCUSSION

Probes To Quantify Urea-Dependent Unfolding of TetR-(D). We analyzed the thermodynamic stability of the sequence variant TetR(D). Urea-dependent unfolding was observed by the changes of fluorescence originating from two Trp residues and the CD reflecting the high content of α helices (Figure 1). Excitation of TetR(D) shows a fluorescence emission maximum at 345 nm (Figure 2a; *17*, *27*). This fluorescence originates mainly from the residues W43, located at the edge of the helix−turn−helix DNA-binding motif, and W75, buried inside the protein core. Denaturation with 8 M urea causes a decrease of the fluorescence intensity and a shift of the emission maximum to 360 nm (Figure 2a), which results from the alteration of solvent accessibility and is typical for protein unfolding (*28*, *29*). We observed the unfolding reaction at 330 nm, where the largest change of fluorescence occurred (Figure 2a).

As a second probe for the unfolding reaction, we used CD spectroscopy. Native TetR(D) shows two CD minima at 209 and 222 nm (Figure 2b) typical for α-helical proteins. These bands are absent at 8 M urea, indicating the complete loss of secondary structure. Identical results were obtained in all unfolding studies with both methods.

Verifying the Two-State Model of Unfolding. The urea-dependent unfolding of TetR(D) shows a monophasic sigmoidal transition without any indication for stable folding intermediates (Figure 2c). Thus, this TetR dimer dissociates and unfolds in a concerted reaction, indicating that folded monomers are unstable. As expected for a bimolecular reaction of denaturation, a 5-fold higher protein concentration stabilizes the native form (Table 1).

The urea-induced unfolding of TetR(D) is a reversible reaction, as is demonstrated by an unfolding/refolding cycle. After unfolding in 8 M urea and subsequent refolding, the fluorescence emission spectrum of TetR(D) was identical with the one of the native protein (Figure 2a). Titration of the refolded protein with atc reveals about 95% activity of inducer binding, and the CD spectrum of the refolded protein is identical with the one of native TetR(D) (Figure 2b). Thus, denaturation under these conditions is reversible, and the results can be interpreted by a two-state model (*28*) in which only folded dimers and unfolded monomers exist in significant concentrations at equilibrium.

Free Energy of Unfolding of TetR(D). Dimeric proteins show generally higher thermodynamic stabilities compared to those of monomeric proteins (*2*), resulting from the energy contributed by the interactions of the subunits (*2*). Extrapolation of the unfolding curve of TetR(D) (Figure 2c) to 0 M urea allows for the calculation of the Gibbs free energy of unfolding $\Delta G°_U(H_2O)$ of 60 kJ mol^{-1} (Table 1). Denaturation of TetR(B) performed here under the same conditions reconfirmed the previously reported stability of 75 kJ mol^{-1} (*17*; Table 1). Thus, TetR(D) is less stable than TetR(B) by 15 kJ mol^{-1} . While the range of these stabilities is typical for this size of dimeric proteins, e.g., the 209 aa CRP has a $\Delta G°_U(H_2O)$ of 80 kJ mol^{-1} (*17*), the difference between the two TetR alleles is surprising. The high sequence identity of 63% amino acids (Figure 1b) motivated us to ask the question if specific residues would be responsible for this marked difference in thermodynamic stability. To address this question, we constructed and purified TetR(B/D) hybrid proteins.

Activities and Thermodynamic Stabilities of TetR(B/D) Hybrid Proteins. We first tested the role of the dimerization surface by exchanging the region from α7 (residue 123) to the C terminus of TetR. Like most other hybrid TetR proteins constructed and analyzed here, this variant is completely inducible in vivo, showing that it is fully functional (Table 2). It exhibits TetR(D) stability, as is indicated by the midpoint of denaturation at a $urea_{1/2}$ concentration of 3.8 M. We then constructed four new chimera and used one

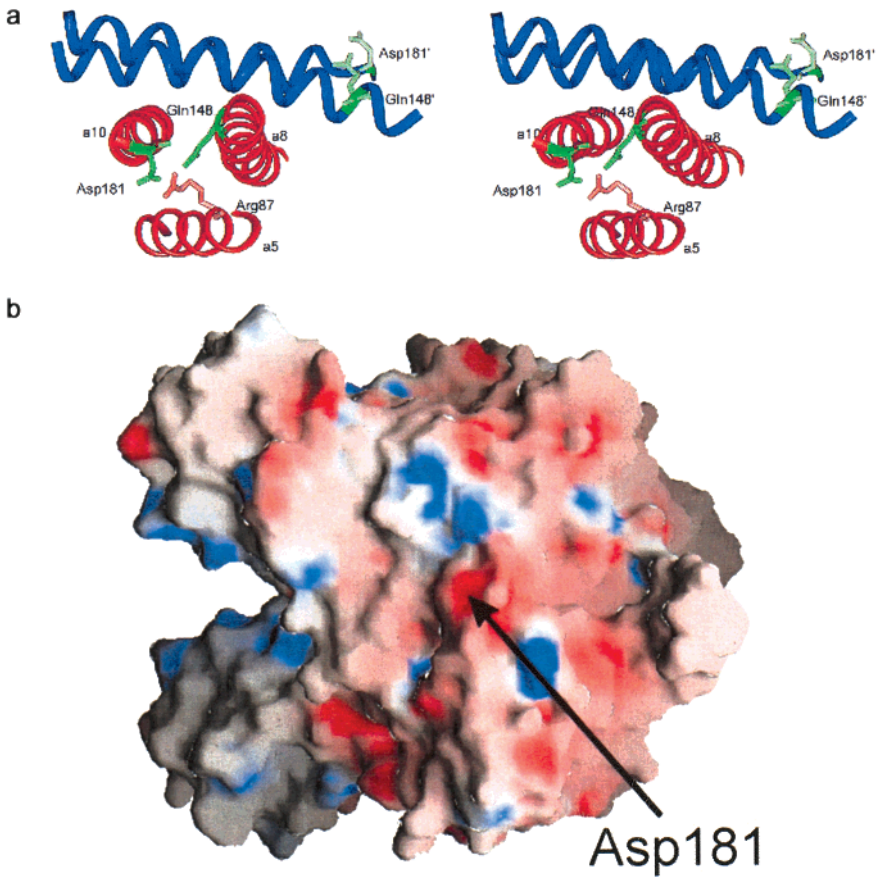

FIGURE 4: Location and potential interactions of the stability determinant in the four-helix bundle. (a, top) Stereoview of the TetR four-helix bundle and the neighboring α-helix 5. The α helices of one subunit are shown in blue, and the ones of the other subunit are shown in red. The side chains of the residues Asp181 and Gln148 are shown for both subunits in green, whereas the side chain of Arg87 is only shown for the red monomer in pink. (b, bottom) Surface potential of TetR showing negative (red) and positive (blue) charge distribution created by using GRASP (*35*). The position of Asp181 is marked by an arrow.

TetR(B/D) chimera from a previous study (*8*; as is shown in Figure 3a) to narrow down the region, altering the thermodynamic stability. The in vivo repression and induction activities determined at 28 °C indicate that TetR(D) is a weak repressor, showing only 8-fold repression, and is also less well inducible than TetR(B). Although the hybrid proteins show a slightly lower inducibility compared to that of TetR(D) (see Table 2), they are sufficiently functional to justify their in vitro analysis. For this purpose, the TetR(B/D) variants were overexpressed and purified as described before (*22*). The purified hybrid proteins were >90% active as determined by titration with atc (*26*). They show fluorescence emission maxima and CD spectra similar to those of TetR(B) and TetR(D) (not shown), suggesting that they adopt the same structure.

The denaturation pathways of all hybrid proteins are sigmoidal and monophasic like the two wild types. The $urea_{1/2}$ values are shown in Table 2. The chimera TetR(B/D)110−208 up to TetR(B/D)179−208 show stabilities similar to those of TetR(D), whereas TetR(B/D)188−208 and TetR(B/D)192−208, on the other hand, exhibit stabilities like that of TetR(B). Thus, the sequence determinant for the thermodynamic stability difference between TetR(B) and TetR(D) must be located between positions 179 and 187. We systematically analyzed the effects of exchanges of fewer amino acids in this region to identify the individual residues important for stability.

Mapping Stability Determinants between Positions 179 and 187. The residues 179−187 form the loop between α9 and α10 and the first two residues of α10 (Figure 1a,b). Because the stability difference should arise from sequence alterations, the conserved residues at positions 183 and 185−187 should have no effect. We started from the hybrid TetR(B/D)179−184 (*9*) and stepwise reduced the TetR(D) portion by constructing TetR(B/D)180−184, TetR(B/D)181−184, TetR(B/D)182−184, and TetR(B/D)184. All variants show repression like TetR(B), show in vivo inducibilities with atc like TetR(D) (Table 2), and have the same fluorescence and CD spectra as TetR(B) or TetR(D) (not shown). Their thermodynamic stabilities were determined from urea-dependent unfolding and analyzed using the two-state model. The results are also shown in Table 2. The hybrids TetR(B/D)179−184, TetR(B/D)180−184, and TetR(B/D)181−184 are as stable as TetR(B), whereas the variants TetR(B/D)182−184 and TetR(B/D)184 show an increased stability of about 4.9 M $urea_{1/2}$ (Table 2). Thus, the Pro to Gln exchange at position 184 stabilizes the protein, indicating that Pro at the second N-terminal position does not stabilize this helix, as was shown in several other cases (*30*). Because the largest stabilization is only seen in TetR(B/D)184 and TetR(B/D)182−184, but not in TetR(B/D)181−184, the exchange of Gly to Asp at position 181 must destabilize the protein. Thus, we have identified two residues in this region which have opposite effects on the stability of TetR. The

residues at position 184 contribute to subunit recognition and might affect stability via interaction between the monomers (*9*) rather than the intrinsic stability of each subunit.

Noninvolvement of Residue 181 in Subunit Recognition of TetR. Because the residue at position 181 influences the stabilities of TetR variants, we constructed the mutants TetR(B/D)181 and TetR(D/B)181 to study the effect of mutual single residue exchanges. Both mutants show repression and inducibilities with atc like their respective TetR wild-type proteins (Table 2) and share the same spectroscopic properties (not shown). The exchanges shift the thermodynamic stabilities of the mutants to the level of the respective other TetR variant (Figure 3b). Therefore, the residue at position 181 is solely responsible for the stability difference between TetR(B) and TetR(D). According to the crystal structure, it is located at the edge of the four-helix bundle and exposed on the surface of the protein, where it is not involved in forming the dimerization interface of TetR (*8*). Because earlier studies revealed that α-helix 10 harbors determinants for the dimerization specificity of TetR (*8*), we nevertheless checked the influence of the exchanges at position 181 on the subunit. The dimerization efficiencies determined using negative transdominant mutants show no change in homo- or heterodimerization (*8*) for TetR(B/D)-181 and TetR(D/B)181 (data not shown). Therefore, we conclude that the different stabilities do not result from an altered recognition of the subunits.

Structural Interpretation of the Stability Effects Exerted by Residue 181. The crystal structures indicate that the residues Asp181 and Asp181′ are located on opposite sides of TetR (Figure 4a). Thus, no direct charge repulsion would occur between these side chains, as was the case for two Glu residues, which led to destabilization of the cold shock proteins Bs-CspB and Bc-Csp (*30*). To investigate whether the alteration of the size of Asp vs Gly may play a role for stability, we checked the crystal structure for potential sterical hindrances or specific repulsions which may be relieved by the exchange of Asp181 to Gly. Only Gln148 and Arg87 in α-helix 8 and α-helix 5, respectively, are close enough to potentially cause a steric or electrostatic repulsion (Figure 4a). To probe this possibility, we constructed the loss-of-contact mutant TetR(D)Q148A. This mutation has the same thermodynamic stability as TetR(D) (see Table 2); hence, Gln148 does not influence stability, and there is no indication for a direct sterical or electrical interference caused by Asp181. The charge distribution surrounding Asp181 is shown in Figure 4b. The last residue of α9 (Asp178), the turn containing the charged residues Asp180 and Asp181, and the first residue of α10 (Glu183) form a cluster of negative charges. The Asp181−Gly exchange leads to a reduction of the negative charge density, which would be expected to increase the stability of that mutant (*31*).

Alternatively, the stabilization resulting from the replacement of Asp181 by Gly could also be due to less direct effects. Asp181 is localized in a turn but assumes dihedral angles of $\Phi = -77°$ and $\Psi = 7°$, which indicate no strain on this residue. Similar angles are found for an Asp residue in a turn of the four-helix bundle protein Rop, the replacement of which by Gly also leads to an extremely thermostable mutant (*32*). Presumably, Gly residues can fit more easily into a left-handed helical backbone. This would indicate that the exchange of Asp181 to Gly leads to more degrees of freedom in the polypeptide chain, allowing the turn to adopt a more relaxed conformation. A similar effect was observed for an Asp to Gly exchange in the turn of the α-spectrin SH3 domain (*33*).

Taken together, our findings demonstrate that residues involved in subunit recognition and recognition motif architecture contribute to the thermodynamic stability of the TetR dimer. Functionally important residues tend to be conserved in sequence variants. Surface-exposed residues are generally not conserved. Nevertheless, we show here that they may be quite important for stability and thereby indirectly influence the function of a protein, e.g., temperature sensitivity.

ACKNOWLEDGMENT

We thank Marco Reich for help with purification of TetR, Dr. Christian Berens and Oliver Scholz for critically reading the manuscript, and Kirsten Oliva for typing the manuscript.

REFERENCES

1. Jones, S., and Thornton, J. M. (1996) *Proc. Natl. Acad. Sci. U.S.A. 93*, 13−20.
2. Neet, K. E., and Timm, D. E. (1994) *Protein Sci. 3*, 2167−2174.
3. Xu, D., Lin, S. L., and Nussinov, R. (1997) *J. Mol. Biol. 265*, 68−84.
4. O'Shea, E. K., Rutkowski, R., and Kim, P. S. (1989) *Science 243*, 538−542.
5. Lin, S. L., Tsai, C. J., and Nussinov, R. (1995) *J. Mol. Biol. 248*, 151−161.
6. Lassalle, M. W., Hinz, H. J., Wenzel, H., Vlassi, M., Kokkinidis, M., and Cesareni, G. (1998) *J. Mol. Biol. 279*, 987−1000.
7. Hefford, M. A., Dupont, C., MacCallum, J., Parker, M. H., and Beauregard, M. (1999) *Eur. J. Biochem. 262*, 467−474.
8. Schnappinger, D., Schubert, P., Pfleiderer, K., and Hillen, W. (1998) *EMBO J. 17*, 535−543.
9. Schnappinger, D., Schubert, P., Berens, C., Pfleiderer, K., and Hillen, W. (1999) *J. Biol. Chem. 274*, 6405−6410.
10. Hillen, W., and Berens, C. (1994) *Annu. Rev. Microbiol. 48*, 345−369.
11. Levy, S. B., McMurry, L. M., Barbosa, T. M., Burdett, V., Courvalin, P., Hillen, W., Roberts, M. C., Rood, J. I., and Taylor, D. E. (1999) *Antimicrob. Agents Chemother. 43*, 1523−1524.
12. Hinrichs, W., Kisker, C., Duvel, M., Muller, A., Tovar, K., Hillen, W., and Saenger, W. (1994) *Science 264*, 418−420.
13. Orth, P., Cordes, F., Schnappinger, D., Hillen, W., Saenger, W., and Hinrichs, W. (1998) *J. Mol. Biol. 279*, 439−447.
14. Orth, P., Schnappinger, D., Hillen, W., Saenger, W., and Hinrichs, W. (2000) *Nat. Struct. Biol. 7*, 215−219.
15. Kisker, C., Hinrichs, W., Tovar, K., Hillen, W., and Saenger, W. (1995) *J. Mol. Biol. 247*, 260−280.
16. Otwinowski, Z., Schevitz, R. W., Zhang, R. G., Lawson, C. L., Joachimiak, A., Marmorstein, R. Q., Luisi, B. F., and Sigler, P. B. (1988) *Nature 335*, 321−329.
17. Backes, H., Berens, C., Helbl, V., Walter, S., Schmid, F. X., and Hillen, W. (1997) *Biochemistry 36*, 5311−5322.
18. Brent, R., and Ptashne, M. (1981) *Proc. Natl. Acad. Sci. U.S.A. 78*, 4204−4208.
19. Wissmann, A., Baumeister, R., Muller, G., Hecht, B., Helbl, V., Pfleiderer, K., and Hillen, W. (1991) *EMBO J. 10*, 4145−4152.
20. Altschmied, L., Baumeister, R., Pfleiderer, K., and Hillen, W. (1988) *EMBO J. 7*, 4011−4017.
21. Berens, C., Pfleiderer, K., Helbl, V., and Hillen, W. (1995) *Mol. Microbiol. 18*, 437−448.
22. Ettner, N., Muller, G., Berens, C., Backes, H., Schnappinger, D., Schreppel, T., Pfleiderer, K., and Hillen, W. (1996) *J. Chromatogr., A 742*, 95−105.

23. Landt, O., Grunert, H. P., and Hahn, U. (1990) *Gene 96*, 125−128.
24. Smith, L. D., and Bertrand, K. P. (1988) *J. Mol. Biol. 203*, 949−959.
25. Miller, J. H. (1992) *Cold Spring Harbor Laboratory*, pp 72−74, Cold Spring Harbor, New York.
26. Takahashi, M., Degenkolb, J., and Hillen, W. (1991) *Anal. Biochem. 199*, 197−202.
27. Hansen, D., Altschmied, L., and Hillen, W. (1987) *J. Biol. Chem. 262*, 14030−14035.
28. Pace, C. N., Shirley, B. A., and Thomson, J. A. (1989) in *Protein structure: A practical approach* (Creighton, T. E., Ed.), pp 311−330, IRL Press at Oxford University Press, Oxford, U.K.
29. Schmid, F. X. (1989) in *Protein Structure: A practical approach* (Creighton, T. E., Ed.), pp 251−285, IRL Press at Oxford University Press, Oxford, U.K.
30. Perl, D., Mueller, U., Heinemann, U., and Schmid, F. X. (2000) *Nat. Struct. Biol. 7*, 380−383.
31. Spector, S., Wang, M., Carp, S. A., Robblee, J., Hendsch, Z. S., Fairman, R., Tidor, B., and Raleigh, D. P. (2000) *Biochemistry 39*, 872−879.
32. Predki, P. F., Agrawal, V., Brunger, A. T., and Regan, L. (1996) *Nat. Struct. Biol. 3*, 54−58.
33. Martinez, J. C., Pisabarro, M. T., and Serrano, L. (1998) *Nat. Struct. Biol. 5*, 721−729.
34. Humphrey, W., Dalke, A., and Schulten, K. (1996) *J. Mol. Graphics 14*, 33−38.
35. Nicholls, A., Sharp, K. A., and Honig, B. (1991) *Proteins*: *Struct., Funct., Genet. 11*, 281−296.

BI001927E